Loss of ATAC-specific acetylation of histone H4 at Lys12 reduces binding of JIL-1 to chromatin and phosphorylation of histone H3 at Ser10

Anita Ciurciu[1], Orban Komonyi[2] and Imre M. Boros[1,2,*]

[1]Institute of Biochemistry, Biological Research Center, Temesvári krt. 62, H-6726 Szeged, Hungary
[2]Chromatin Research Group of HAS, Department of Biochemistry and Molecular Biology, University of Szeged, Közép fasor 52, H-6726 Szeged, Hungary
*Author for correspondence (e-mail: borosi@bio.u-szeged.hu)

Accepted 24 June 2008
Journal of Cell Science 121, 3366-3372 Published by The Company of Biologists 2008
doi:10.1242/jcs.028555

Summary

Various combinations of post-translational modifications of the N-terminal tails of nucleosomal histones serve as signals to govern chromatin-related processes. The relationship, however, among different types of histone modifications – most frequently acetylation, phosphorylation and methylation – and the order of their establishment has been explored only in a few cases. Here we show that a reduced level of histone H4 acetylated at Lys12 by the ATAC-HAT complex leads to a decrease in the histone H3 phosphorylation at Ser10 by the kinase JIL-1. As JIL-1 activity antagonizes histone H3 dimethylation at Lys9 by SU(VAR)3-9, our observations demonstrate the interdependent actions of an acetyltransferase, a kinase and a methyltransferase. We demonstrate that, in accord with the steps of modifications, mutations that affect ATAC subunits (such as *dGcn5*, *dAda2a* and *dAda3*) (1) decrease the level histone H3 phosphorylation at Ser10 , (2) can be rescued partially by JIL-1 overproduction, (3) enhance the spread of histone H3 dimethylation at Lys9 and (4) are suppressed by mutations of *Su(var)3-9*. We propose that a reduced level of histone H4 acetylated at Lys12 by ATAC attenuates histone H3 phosphorylation at Ser10 by JIL-1 owing to reduced binding of JIL-1 to hypoacetylated chromatin.

Supplementary material available online at
http://jcs.biologists.org/cgi/content/full/121/20/3366/DC1

Key words: Histone acetylation, Histone phosphorylation, ATAC, JIL-1, SU(VAR)3-9, GCN5, ADA2

Introduction

Post-translational modifications of the N-terminal tails of nucleosomal core histones provide important means of regulating chromatin structure and processes that involve chromatin in eukaryotic cells. The different types of covalent histone modifications can cause structural alterations that make the chromatin more accessible or, by contrast, result in a tighter packaging of nucleosomes (Ito, 2007; Li et al., 2007; Oki et al., 2007). Interestingly, in some cases the same type of modification on the same residue can have entirely different consequences. An example of this is histone H3 when phosphorylated at Ser10 (H3S10ph), which results in chromatin decondensation and transcription activation at several loci during interphase, but chromatin condensation and gene silencing during mitosis (Johansen and Johansen, 2006; Oki et al., 2007). This suggests that the distribution and the interplay of different types of modification must have a determining role in the final outcome. The interplay of different modifications also has a role in determining affinities by which formation of one type of modification facilitates or inhibits the formation of a subsequent one. It has been observed that phosphorylation of histone H3 at S10 can enhance acetylation of histone H3 at Lys14 (K14) (Cheung et al., 2000; Lo et al., 2000) and inhibit methylation of histone H3 at Lys9 (K9) (Rea et al., 2000). In another example, the acetylation of histone H4 at Lys 12 (K12) was suggested to be required for the methylation of histone H3 at K9 and the following HP1 recruitment to the centromeric regions of *Drosophila* chromosomes (Swaminathan et al., 2005). Crosstalk between histone H3 phosphorylation at S10, and acetylation and methylation thus clearly exists. Acetylation, and similarly, phosphorylation and methylation of specific histone tail residues can be brought about by several distinct enzymes or protein complexes that often have overlapping specificities (Berger, 2007; Lee and Workman, 2007; Li et al., 2007). It is therefore expected that a particular (pre-)established constellation of modifications can have different effects on the establishment of a subsequent modification, depending on the enzymes/complexes participating in the process.

In mutants of several *Drosophila* genes that have roles in histone post-translational modifications, alterations in the higher-order polytene chromosome structures have been observed. Mutations affecting the JIL-1 kinase (Wang et al., 2001), subunits of the NURF chromatin-remodeling complex (*iswi* and *nurf* alleles) (Badenhorst et al., 2002; Badenhorst et al., 2005; Deuring et al., 2000) as well as other chromatin-associated proteins, such as SU(VAR)205 (also known as HP1), SU(VAR)3-7 (Spierer et al., 2005) and Chromator (also known as Chriz) (Eggert et al., 2004; Rath et al., 2006), each result in structural defects of chromatin. The distortions are most clearly seen in the structure of male X chromosomes, resulting in the appearance of a puffed-X morphology, also referred to as ‘bloated male X’ or ‘pompon’ phenotype (Zhimulev, 1996). Under the light microscope the male X seems to be shortened and widened with no coherent banded regions observable. Whether the structural distortions observed by light microscopy in each of the above mutants reflect identical changes in molecular alterations or are the results of different changes is at present unclear. An altered level of acetylation of histone tails, however, clearly can have a role in

the appearance of the bloated male X chromosome, as indicated by the dependence of this phenotype of *Su(var)3-7* and *Nurf301* mutants on the presence of a functional dosage-compensation complex (Carre et al., 2007; Spierer et al., 2005). It is believed that hyperacetylation of K16 in histone H4 at male X chromosomes (which ensures a twofold higher transcription level compared with the X chromosomes of females) by the MOF acetyltransferase, makes the male X chromosome prone to structural distortions.

The histone kinase JIL-1 localizes specifically to euchromatic interband regions of polytene chromosomes (Jin et al., 1999). JIL-1 phosphorylates histone H3 at S10 and a reduction in JIL-1 level results in the spreading of histone H3 dimethylated at Lys9 (H3K9me2) to ectopic locations (Zhang et al., 2006). A reduced level of JIL-1 also leads to a global disruption of chromosome structure (Deng et al., 2008; Jin et al., 2000; Wang et al., 2001; Zhang et al., 2003). In the polytene chromosomes of *JIL-1*-mutant flies the tight parallel alignment of chromatids is disrupted. The altered appearance of the male X chromosomes in *JIL-1*-mutant flies is believed to be the result of an increased dispersal of the chromatin into a diffuse network (Deng et al., 2005).

ADA2a, ADA3 and GCN5 (KAT2) are constituents of the Ada2a-containing (herafter referred to as ATAC) histone acetyltransferaste (HAT) complex (Guelman et al., 2006) that specifically acetylates histone H4 at Lys5 and Lys12 (K5 and K12, respectively) (Ciurciu et al., 2006). In *dAda2a*, *dAda3* and *dGcn5* mutants we observed an altered chromosome structure, similar to that seen in *Nurf301* and *JIL-1* mutants (Carre et al., 2007; Ciurciu et al., 2006; Grau et al., 2008). These structural alterations were observed most clearly on the male X chromosomes and resulted in a bloated X phenotype. Since chromosome structural defects were not observed in Spt-Ada-Gcn5 (SAGA)-HAT-complex-specific *dAda2b* mutants (Pankotai et al., 2005) we set out to test whether the similar phenotypes of *JIL-1*- and ATAC-mutant chromosomes reflect a functional interaction that might exist between the ATAC-HAT complex and JIL-1 kinase, but not between the SAGA-HAT complex and JIL-1 kinase. Here, we present evidence that in ATAC mutants the localization of JIL-1 kinase to chromatin and the histone H3 phosphorylation at S10 are substantially reduced. Furthermore, we demonstrate genetic interactions between ATAC and *JIL-1*, and *Su(var)3-9* alleles. On the basis of these data we propose that acetylation of histone H4 at K12 by ATAC facilitates JIL-1-dependent phosphorylation of histone H3 by augmenting JIL-1 binding to chromatin.

Results

The level of H3S10ph is decreased in mutants deficient in ATAC function

To determine whether a dependence between JIL-1 and ATAC functions exist we studied the levels of histone H4 acetylated at K12 (H4K12ac; ATAC-dependent formation) and histone H3 phosphorylated at S10 (H3S10ph; JIL-1-dependent formation) in *JIL-1* and ATAC subunit mutants. Immunoblots developed with antibodies specific for K12-acetylated H4 demonstrate dramatically decreased levels of H4K12ac in total protein extracts of *dAda2a* and *dGcn5* mutants, whereas the levels of H4K12ac in *dAda2b* and *JIL-1* mutants is similar to those observed in the wild-type sample (Fig. 1A). By contrast, the levels of H3S10ph, as determined by immunoblotting using antibodies specifically against H3S10ph, is greatly reduced in *dAda2a* and *dGcn5* mutants, but were comparable with those in the controls of the SAGA-specific *dAda2b* mutant samples (Fig. 1B). Similarly, in *dAda3* mutants, we also detected

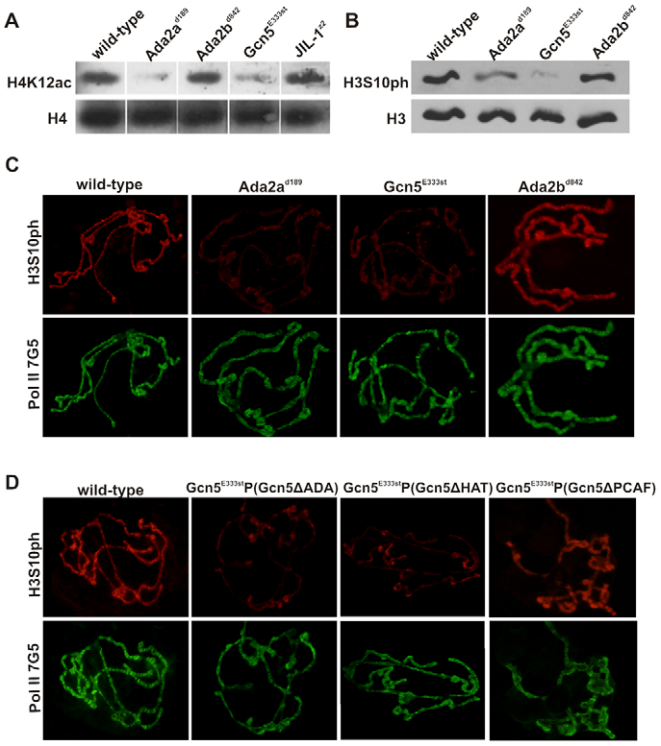

Fig. 1. Decreased level of ATAC-specific H4 acetylation results in reduced phosphorylation of histone H3 at S10. (A) Immunoblots of total protein extracts of wild-type (w^{1118}), *dAda2a*^{d189}, *dAda2b*^{d842}, *dGcn5*^{E333st} and *JIL-1*^{z2} late third-instar larvae developed with antibodies specifically recognizing H4K12ac (top), and H4 (bottom). (B) Immunoblots of total protein extracts of wild-type (w^{1118}), *dAda2a*^{d189}, *dGcn5*^{E333st} and *dAda2b*^{d842} late third-instar larvae developed with antibodies specific for H3S10ph (top), and for H3 (bottom). In A and B, the same membranes shown on the top were reprobed with H3- or H4-specific antibodies. (C) Double labeling with antibodies specific for H3S10ph (top) and for the C-terminal domain of the largest subunit of RNA polymerase 2 (Pol II 7G5; bottom) of polytene squashes from wild-type, *dAda2a*^{d189}, *dAda2b*^{d842}, *dGcn5*^{E333st} larvae. (D) Polytene chromosome squashes of *dGcn5*-null (*dGcn5*^{E333st}) third-instar larvae expressing a mutated *dGcn5* transgene as indicated, double stained with antibodies specific for H3S10ph (top) and for the C-terminal domain of the largest subunit of RNA polymerase II (Pol II 7G5; bottom).

a substantial decrease in the level of H3S10ph (data not shown) (Grau et al., 2008). Immunostaining of salivary gland polytene chromosomes of *dGnc5* and *dAda* mutants corroborate the results of immunoblots in that the staining intensity displayed with H3S10ph-specific antibodies used for both *dAda2a* and *dGcn5* chromosomes is greatly reduced compared with wild type or *dAda2b* chromosomes (Fig. 1C). Again, polytene chromosomes of *dAda3* mutants displayed staining of similar intensity compared with mutants of other ATAC components. In contrast to the observed decrease in H3 phosphorylation of polytene chromosomes, we did not observe differences in the staining intensity of mitotic chromosomes in the neuroblasts of ATAC-mutant and wild-type larvae (data not shown). We thus concluded that in the absence of a functional ATAC-HAT complex the level of JIL-1-specific H3 phosphorylation is severely reduced.

The acetyltransferase activity of the ATAC-HAT complex is due to GCN5 (KAT2), although the existence of other ATAC-HAT subunits with catalytic activity has also been suggested (Guelman et al., 2006; Suganuma et al., 2008). Previously we have shown

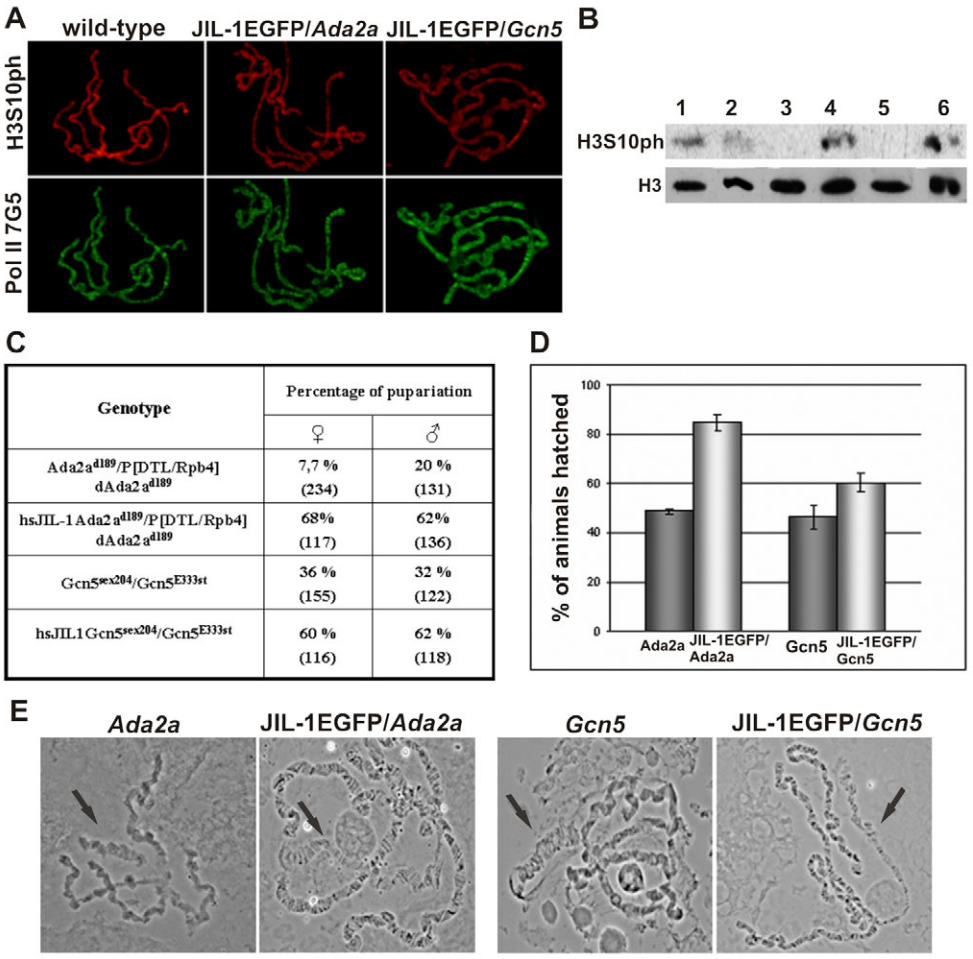

Fig. 2. Ectopic expression of *JIL-1* from a transgene in ATAC subunit mutants restores levels of H3S10ph, increases the survival of ATAC mutants and improves male X chromosome structure. (A) Polytene chromosome squashes of wild-type, and JIL-1 transgene expresser $dAda2a^{d189}$ and $dGcn5^{E333st}$ ($JIL\text{-}1EGFP/dAda2a^{d189}$ and $JIL\text{-}1EGFP/dGcn5^{E333st}$) third-instar larvae double stained with H3S10ph-specific (top) and Pol II-specific (bottom) antibodies. (B) Immunoblot of total protein extracts of (1) wild-type, (2) *JIL-1EGFP*, (3) $dAda2a^{d189}$, (4) $JIL\text{-}1EGFP/dAda2a^{d189}$, (5) $dGcn5^{E333st}$ and (6) $JIL\text{-}1EGFP/dGcn5^{E333st}$ third-instar larvae developed with H3S10ph- (top) and H3-specific (bottom) antibodies. (C) Lethal phases of $dAda2a^{d189}$, $JIL\text{-}1EGFP/dAda2a^{d189}$, $dGcn5^{E333st}$ and $Jll\text{-}1EGFP/dGcn5^{E333st}$ animals. The percentages of animals perishing in the indicated stages are shown. Numbers of third instar larvae of the particular genotype and sex are given in parentheses. The sex of the animals was determined by observing the presence of testes in L3. (D) The hatching rate of hypomorph *dAda2a* and *dGcn5* mutants in the absence and the presence of a JIL-1EGFP transgene. The genotypes are described in Materials and Methods. Numbers of animals studied were 625 *dAda2a* hypomorph, 456 *Gcn5* hypomorph as controls, 781 *dAda2a* and 488 *dGcn5* carrying JIL-1 transgene. (E) Phase-contrast images of $dAda2a^{d189}$, $JIL\text{-}1EGFP/dAda2a^{d189}$, $dGcn5^{E333st}$ and $Jll\text{-}1EGFP/dGcn5^{sex204/E333st}$ polytene chromosomes of late third-instar male larvae. Arrows indicate the male X chromosomes.

that the loss of GCN5 activity results in a dramatic decrease in the levels of H4K5ac and H4K12ac (Ciurciu et al., 2006). We therefore found it interesting to determine whether the HAT activity of GCN5 is required to enhance JIL-1-dependent H3 phosphorylation. For this, we studied the levels of H3S10ph in animals in which parts of GCN5 functions were provided by transgenes. Polytene-chromosome-staining of transgene carrier larvae revealed that *dGcn5* transgenes that lack the HAT-catalytic or the ADA2-interacting domain fail to restore levels of H3S10ph in *dGcn5*-null mutants (Fig. 1D). Previously, we have shown that *dGcn5*-null animals that carry these transgenes are defective in acetylation of histone H4 at K5 and K12, whereas a GCN5 transgene that lacks the PCAF-homology region is capable to restore histone H4 acetylation at K5 and K12 (Ciurciu et al., 2006). Similarly, but in contrast to ΔHAT-GCN5 and ΔADA-GCN5 transgenes, phosphorylation of histone H3 at S10 was complemented by the ΔPCAF construct (Fig. 1D). Combined, these data strongly suggest that the loss of ATAC-dependent histone H4 acetylation decreases JIL-1-dependent phosphorylation of H3.

JIL-1 overexpression restores levels of H3S10ph and suppresses phenotypic features of ATAC mutants

The functional failure of ATAC might lead to decreased levels of H3S10ph because H4 tails that contain acetylated K12 have a direct role in the enhancement of JIL-1 function. Alternatively, several indirect mechanisms that alter JIL-1 activity might be triggered by altered chromatin structure. In an attempt to gain information on the underlying mechanism of ATAC and JIL-1 interplay we studied the effect of ectopic JIL-1 overproduction in ATAC mutants. Expression of the hs83-promoter-driven JIL-1–EGFP transgene (herafter referred to as JIL-1EGFP transgene) in *dAda2a* and *dGcn5* mutants restored histone H3S10ph levels to essentially normal levels (Fig. 2A,B), and decreased the effects of ATAC subunit mutations that lead to either lethal phase or chromosome structural distortions (Fig. 2C-E). *dAda2a*- or *dGcn5*-null mutants, which live for about 14 days in L3 stage, do not evert spiracle and have a lethal phase in late third-instar larval stage; upon JIL-1 overproduction spiracle were evert and pupae formed with high frequency (Fig. 2C). Similarly, ectopic expression of JIL-1 increased the survival of hypomorph *dAda2a* or *dGcn5* mutants, as shown by increased hatching of flies with the JIL-1-transgene carrier *dAda2a* or *dGcn5*, compared with the number of animals without a JIL-1 transgene (Fig. 2D). Since JIL-1 has been implicated in dosage compensation (Jin et al., 2000) we determined whether overproduction of JIL-1 affects males and females differently; we observed no rescue differences between the two sexes. The effect of JIL-1 overproduction can also be observed well in the change of the chromosome structure of ATAC mutants. The bloated phenotype of male X chromosomes characteristic for each ATAC mutant studied (*dAda2a*, *dAda3* and *dGcn5*) is substantially suppressed when JIL-1 is overproduced (Fig. 2E). We noticed a less striking but clearly observable improvement in the structure of autosomes

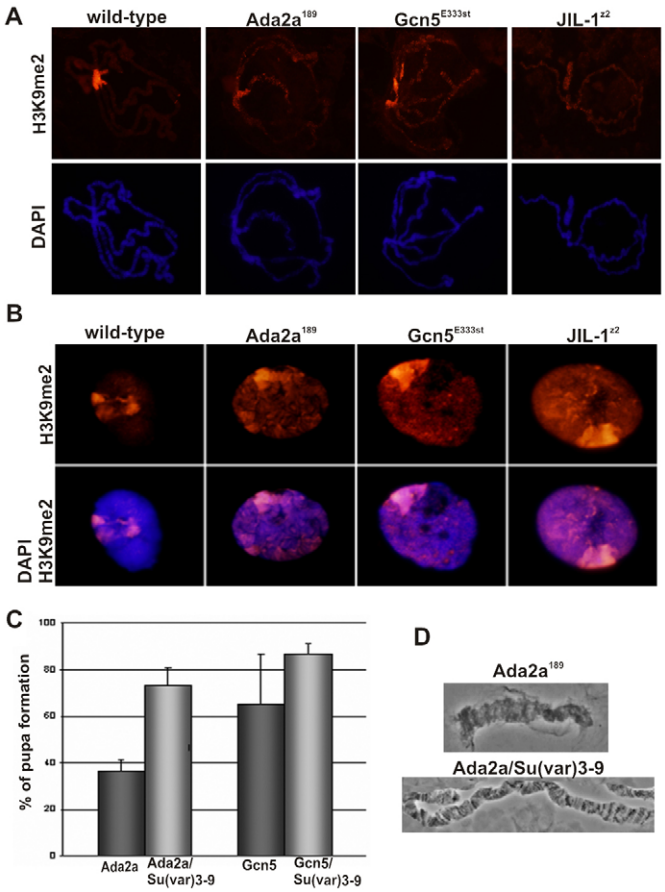

Fig. 3. Ectopic spreading of H3K9me2 in *dAda2a*, *dGcn5* and *JIL-1* mutants. (A) Polytene chromosome squashes of *dAda2a*^{d189}-, *dGcn5*^{E333st}- and *JIL-1*^{z2}-null homozygous third-instar larvae stained with H3K9me2-specific antibody and DAPI (blue). (B) Polytene nuclei of *dAda2a*^{d189}-, *dGcn5*^{E333st}- and *JIL-1*^{z2}-null homozygous larvae stained with H3K9me2-specific antibody (red) and DAPI (blue). (C) *Su(var)3-9* heterozygocy increases the viability of *dAda2a*- or *dGcn5*-null animals. The percentages of animals perishing at the indicated developmental stages are shown. The number of animals in each category was over 350. (D) *Su(var)3-9* heterozygous background improves the structure of male X chromosomes of *dAda2a*-null mutants.

in both males and females in JIL-1-overexpressing ATAC mutants (Fig. 2E and data not shown). Thus, these data strongly suggest that the similar chromatin-structure distortions seen both in ATAC and *JIL-1* mutants, but most clearly in the structure of the male X chromosome, are – at least in part – owing to the identical underlying cause: reduced levels H3S10ph. Furthermore, the suppressive effect that JIL-1 overproduction exerts on the phenotype of ATAC mutants also suggests that the reduced levels of ATAC-specific acetylation of histone H4 at K5 and K12 does not prevent, but only hinders JIL-1-dependent phosphorylation of histone H3S10.

Mutations of ATAC subunits enhance the spreading of histone H3 dimethylation at K9 by SU(VAR)3-9

As phosphorylation of histone H3 at S10 by JIL-1 was reported to counteract histone H3 dimethylation of K9 and heterochromatin formation, we reasoned that if ATAC mutations indeed hinder JIL-1 function, then an increased level of H3 dimethylated at K9 (H3K9me2) should be observed in ATAC mutants; moreover, mutations of *Su(var)3-9* (the gene encoding the dimethyltransferase dimethylating H3 at K9) (Schotta et al., 2002; Tschiersch et al., 1994) should overcome the effect of ATAC mutations. To test this assumption we examined H3K9me2 levels in ATAC mutants and studied the phenotype of *dAda2a/Su(var)3-9* and *dGcn5*/*Su(var)3-9* double mutants. Immunostaining of polytene chromosome spreads using H3K9me2-specific antibodies revealed a spread of signal on *dAda2a* and *dGcn5* mutant chromosomes similarly to that observed on *JIL-1* chromosomes (Fig. 3A,B). We observed a similar extent of H3K9me2 spreading in *dAda3* mutants also (data not shown). Whereas on samples of the control strain (w^{1118}) the H3K9me2-positive signal is detectable mostly at centromeric regions, on the fourth chromosomes and as a few bands on autosomes, on *dAda2a*, *dGcn5* and *dAda3* chromosomes the staining on the autosome arms in both males and females is readily detectable (Fig. 3A). The spreading of H3K9 dimethylation in ATAC mutants is even more obvious in 'smush' preparations (Fig. 3B). For testing the genetic interaction between *Su(var)3-9*- and ATAC-subunit mutants we studied the effect of *dAda2a* and *dGcn5* deficiency in *Su(var)3-9*^{1} and *Su(var)3-9*^{2} heterozygous backgrounds. Because both *Su(var)3-9* and *dAda2a* or *dGcn5* are located on the third chromosome, we first recombined the *Su(var)3-9*^{1} or *Su(var)3-9*^{2} allele onto *dAda2a*^{d189} or *dGcn5*^{sex204}. Subsequently, *Su(var)3-9 dAda2a*^{189}/TM6C or *Su(var)3-9 dGcn5*^{sex204}/TM6C animals were crossed to *P[DtlRpb4] dAda2a*^{d189}/TM6C and *dGcn5*^{E333st}/TM6C generating *Su(var)3-9 dAda2a*^{189}/*P[DtlRpb4] dAda2a*^{d189} or *Su(var)3-9 dGcn5*^{sex204}/*dGcn5*^{E333st} progeny homozygous for *dAda2a* or *dGcn5* mutation and heterozygous for *Su(var)3-9*. Both of these *Su(var)3-9* alleles are null (Ebert et al., 2004) and gave the same results, such that a decreased level of SU(VAR)3-9 increased the survival of ATAC mutants, permitting development to P4-P5 stages in high frequency and up to pharate adult stage in small numbers (Fig. 3C). Also, *Su(var)3-9* heterozygosis improved the chromosome structure of ATAC mutants (Fig. 3D).

Loss of acetylation of H4 at K12 decreases JIL-1 localization to chromatin

The reason for the reduced phosphorylation levels of histone H3 at S10 in mutants whose ATAC subunits were affected could be that *JIL-1* is one of the numerous genes downregulated when histone H4 is not acetylated at K12 and low levels of JIL-1 cannot sustain normal phosphorylation levels of histone H3 at S10. To test this possibility we studied the expression of *JIL-1* in ATAC mutants. First, we compared *JIL-1* mRNA levels in *JIL-1*, *JIL-1*/+, *dGcn5*, *dAda2a* and *dAda3* mutants and w^{1118} controls by quantitative real-time PCR (Q-RT-PCR) (Fig. 4A). In all three ATAC mutants tested we found the level of *JIL-1* mRNA to be slightly decreased, corresponding to ~approximately 60% of the control samples. As expected, in homozygous *JIL-1*-null mutants we detected a dramatic decrease in the level of specific message, whereas in *JIL-1*/+ heteroallelic combinations, which display the wild-type phenotype, *JIL-1* mRNA was detected at a levels similar to those in ATAC mutants, corresponding to 60% of wild-type levels. Next, we compared the JIL-1 protein levels in wild-type, *dAda2a* and *dAda2b* samples by immunoblots and found that JIL-1 was present at similar levels in total protein extracts of all three samples (Fig. 4B). By immunostaining tissue samples with JIL-1-specific antibody we also found the signal intensities comparable in *dAda2a* or *dGcn5* and wild-type larvae. A comparison of JIL-1-specific staining intensities of wild-type, *JIL-1* and ATAC mutant chromosomes, however, revealed a more-severe decrease in JIL-1 levels within *dAda2a* and

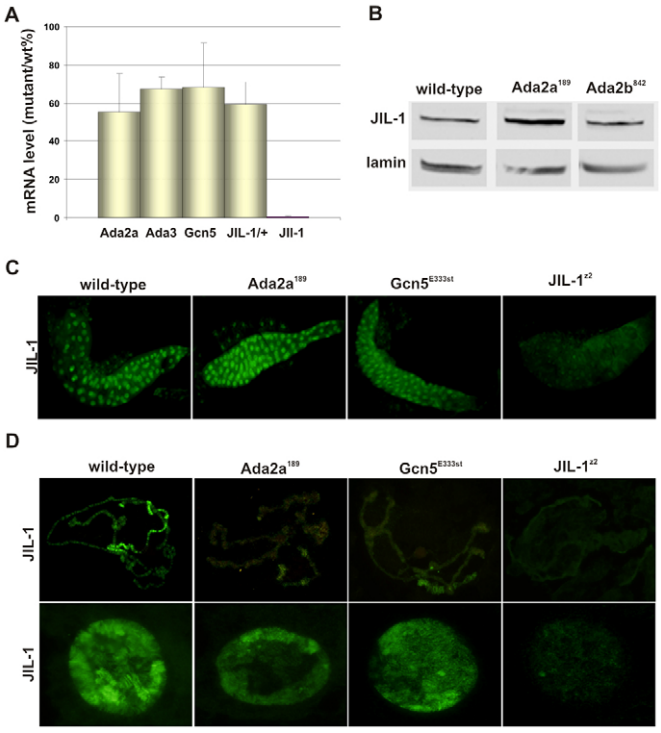

Fig. 4. The level of JIL-1 expression does not, but JIL-1 binding to chromatin is severely decreased in ATAC mutants. (A) The level of *JIL-1* mRNA in ATAC and *JIL-1* mutants determined by real-time RT-PCR. (B) Immunoblot of total protein extracts of $dAda2a^{d189}$- and $dAda2b^{d842}$-null mutant and wild-type third-instar larvae developed using JIL-1-specific antibody. (C) Immunostaining of salivary glands of ATAC- and *JIL-1*-null mutants using JIL-1-specific antibody. (D) Immunostaining of polytene chromosomal spreads (top) and 'smush' preparations (bottom) of wild-type and $dAda2a^{d189}$, $dGcn5^{E333st}$ and $JIL\text{-}1^{z2}$ third-instar larvae using JIL-1-specific antibody. Chromosomes of males are shown. The *JIL-1* mutant shown is null homozygote.

dGcn5 chromosomes (Fig. 4D). Expression of a GCN5 transgene that lacked the PCAF-homology region, but which complemented acetylation of histone H4 at K5 and K12 and phosphorylation of histone H3 at S10 in *dGcn5*-null mutants also restored JIL-1 localization to polytene chromosomes, whereas a GCN5 transgene lacking the HAT domain, which failed to rescue of H4 acetylation and H3 phosphorylation at S10, was also defective in restoring chromosomal localization of JIL-1 (supplementary material Fig. S1). Remarkably, JIL-1 binding to *dAda2a* and *dGcn5* chromosomes is not lost completely and a weak signal all along the chromosome arms and, particularly, on the dosage-compensated male X chromosomes is well discernible (Fig. 4D, top part). The rather gentle 'smush' preparation technique for polytene chromosome staining provided similar results. It is notheworty, that the difference in staining intensity between wild-type and ATAC-mutant samples was repeatedly less on the 'smush' preparations than on the chromosome spreads prepared using harsher conditions. (Fig. 4D; supplementary material Fig. S2, compare top and bottom). By contrast, polytene chromosome spreads and 'smush' preparations of JIL-1 hetrozygotes displayed staining intensities with JIL-1 specific antibody that was indistinguishable from wild-type controls (supplementary material Fig. S2). The substantial difference in JIL-1-specific staining of ATAC mutants was repeatedly observed both in male and female chromosomes (Fig. 4D; supplementary material Fig. S2)

Discussion

In several mutants whose HAT-subunit complexes were affected we observed structural chromatin changes similar to those seen in *JIL-1, Nurf301* and *Su(var)2-5* mutants. Note that, whereas *dAda2a*, *dAda3* and *dGcn5* mutants display distorted chromosome phenotypes, *dAda2b*-null mutants do not. The presence of ADA2a and ADA2b is characteristic for the ATAC and SAGA-HAT complexes, respectively (Ciurciu et al., 2006; Guelman et al., 2006), and we therefore hypothesized that the altered chromatin structure resulted from a failure of the ATAC complex. With the experiments presented here we provide support to this hypothesis and also provide a suggestion as to why reduced levels of H4 acetylation by ATAC leads to chromosome structural alterations. Our data indicate that the chromosome structural defects observed in ATAC mutants are, at least in part, due to a reduced levels of H3S10ph. Ectopic expression of the histone kinase JIL-1 in ATAC mutants restores levels of H3S10ph and also restores the polytene chromosome structure close to normal. This observation suggests that the direct cause of altered chromosome structure is not the lack of H4 acetylation per se, but rather the concomitant loss of H3 phosphorylation in the absence of ATAC function. In agreement with this we observed a substantially reduced level of JIL-1 kinase associated with ATAC-mutant chromosomes. The decreased JIL-1 function in ATAC mutants provides an explanation for the observed genetic interaction between ATAC and *Su(var)3-9* mutants, and for the observation that the histone H3 dimethylation at K9 due to SU(VAR)3-9 extends in ATAC mutants (Deng et al., 2007; Zhang et al., 2006).

We find that JIL-1 kinase expression at low levels is unlikely to be the underlying cause of the severely decreased levels of H3S10ph in ATAC mutants. Several independent observations argue against this. First, we observed only an ~40% reduction of *JIL-1* mRNA levels in ATAC mutants. In the same experiments we found that at JIL-1/+ heteroallelic combinations the *JIL-1* mRNA levels reduced to a similar extent. In contrast with the small difference in *JIL-1* mRNA levels, ATAC mutants showed marked decreases of H3S10ph and JIL-1 localization to chromatin, and displayed the bloated male X chromosome phenotype, whereas *JIL-1*/+ heteroallelic combinations were indistinguishable from wild-type in all in these aspects. Previous studies have also shown that the levels f H3S10ph in *JIL-1*/+ heterozygote are comparable with that in wild-type larvae (Zhang et al., 2006), and that hypomorph *JIL-1* mutants, which produce approximately one-tenth of the normal JIL-1 protein levels, affect the chromosome structure only moderately (Wang et al., 2001). Second, we did not observe a significant reduction in the JIL-1 protein level in ATAC mutants by either immunoblotting or immunostaining of tissue samples. In contrast to this, we repeatedly observed a severely attenuated localization of JIL-1 in the chromatin of ATAC mutants. We therefore favor the idea that JIL-1 protein present in ATAC mutants is functionally restricted and unable to effectively phosphorylate histone H3 at S10. A functional failure of JIL-1 could arise from its altered interaction with chromatin that is hypoacetylated at histone H4 at K5 and K12. Being devoid of these modifications, a less-open chromatin might have restricted accessibility, or the lack of H4K5ac and H4K12ac might have a specific effect on the interaction between JIL-1 and chromatin. Although our present data allow no distinction between these possibilities, we noticed the

preferential association of JIL-1 to the H4K16-hyperacetylated chromatin of the male X chromosomes. The mechanism of JIL-1 binding to H4K16-acetylated chromatin is, however, believed to be owing to its association with dosage-compensation-complex proteins (Jin et al., 2000). Alternatively, a direct interaction between JIL-1 and ATAC complex might also exist.

The relationship of H4 acetylation by ATAC and H3 phosphorylation by JIL-1 has not been observed before, and may seem surprising. JIL-1 is associated primarily with transcriptionally active interband regions, whereas H4K12 acetylation is observed mostly on compacted chromosomal regions (Labrador and Corces, 2003). However, neither JIL-1 nor the ATAC complex reside exclusively at eu- or heterochromatic regions and roles in both chromatin condensation and decondensation have been proposed for both H3S10 phosphorylation and H4K12 acetylation (Berger, 2007; Ito, 2007; Oki et al., 2007; Swaminathan et al., 2005). In ATAC mutants the expression of a large number of genes is substantially altered (Carre et al., 2007; Grau et al., 2008), demonstrating the role of histone H4 acetylation at K5 and K12 in transcription regulation. However, acetylation of histone H4 at K12 has been suggested to have a key role in the formation of heterochromatin following replacement of histone H2Av (Swaminathan et al., 2005). According to this model acetylation of histone H4 at K12 triggers deacetylation and the methylation of histone H3 at K9, which in turn serves as signal for HP1 binding. In contrast to this model, we did not observe that decreasing levels of H4K12ac provoked a decrease in the levels of H3K9me2. By contrast, our data suggest that a change of H4K12ac levels indirectly causes a change in the opposite direction, namely in the levels of H3K9me2, by modulating phosphorylation levels of histone H3 at S10. In accord with our observations, the spread of H3K9me2 in *Jil-1* mutants has been reported previously (Zhang et al., 2006), and a recent report from the Johansen lab (Deng et al., 2008) has nicely demonstrated the possible involvement of JIL-1 in chromatin-structure remodeling. At present, we cannot offer a convincing argument to resolve the discrepancy between these two observations and we assume that, depending on the specific chromosomal regions and – particularly – on the already existing histone modifications, the acetylation of histone H4 at K5 and K12 can have different effects.

The data we present here provide an explanation for the observed bloated male X phenotype in ATAC mutants. Recently, we demonstrated a genetic interaction between mutations that affect subunits of the NURF–chromatin-remodeling and ATAC-HAT complexes, and the interplay between the NURF and the ATAC complexes in chromatin-structure organization. The results of those studies suggested that NURF is required for ATAC to access the chromatin. Here we show that the ATAC function is required for JIL-1 activity, and that in the absence of JIL-1 the SU(VAR)3-9 methyltransferase will gain a greater access to the K9 residue of histone H3, which has also been shown previously (Zhang et al., 2006). Combined, these observations indicate a cascade of interdependent steps in the modification of chromatin structure, involving an ATP-dependent chromatin-remodeling complex, a histone-H4-specific acetyltransferase complex, and the balanced action of a histone-H3-specific kinase and methyltransferase. The bloated male X phenotype, characteristic of mutations that affect either NURF, ATAC or JIL-1, and the genetic interactions among these and, also, with *Su(var)3-9* mutants, as described here and in earlier reports (Zhang et al., 2006), provide a strong support for the in vivo existence of such a cascade.

Materials and Methods

Drosophila stocks, genetic crosses and phenotype analysis

Fly stocks were raised and crosses performed at 25°C on standard medium containing nipagin. The $dAda2a^{d189}$ and $dAda2a^{hyp}$ alleles have been described (Komonyi et al., 2005; Pankotai et al., 2005; Papai et al., 2005). *dGcn5*-null and hypomorph alleles $dGcn5^{E333st}$, $dGcn5^{sex204}$, $dGcn5^{C137T}$ and Gcn5ΔHAT, Gcn5ΔADA and Gcn5ΔPCAF transgenes were kindly provided by Christophe Antoniewski (Institute Pasteur, Paris, France) (Carre et al., 2005). The $dAda3^{2}$ allele has been described previously (Grau et al., 2008).

The $JIL\text{-}1^{Z2}$ allele and the JIL-1-GFP wild-type transgene P(hs83-GFP-JIL-1,w+) were kindly provided by Kristen Johansen (Iowa State University, Ames, IA) (Jin et al., 1999; Wang et al., 2001; Zhang et al., 2003). All alleles were kept as heterozygotes with TM6C, Tb Sb, TM6B, Tb Hu or T(2;3)TSTL, Cy; Tb Hu balancer chromosomes and mutants were selected on the basis of the Tb^{+} phenotype. The $dSu(var)3\text{-}9^{1}$ and $dSu(var)3\text{-}9^{2}$ stocks were obtained from the Bloomington stock center (Reuter et al., 1986; Tschiersch et al., 1994). As control the w^{1118} strain was used (Ryder et al., 2007).

Overexpression of JIL-1 in *dAda2a* and dGcn5 mutant backgrounds was achieved by crossing *P[hs83-GFP-JIL-1]/P[hs83-GFP-JIL-1]*; $dAda2a^{d189}$/*TM6B* to *P[DtlRpb4]* $dAda2a^{d189}$/*TM6C*. The analyzed genotype was *P[hs83-GFP-JIL-1]/+*; $dAda2a^{d189}$/*P[DtlRpb4]* $dAda2a^{d189}$. The animals with the genotype P[hs83-GFP-JIL-1]/+; $Gcn5^{E333st}/Gcn5^{sex204}$ were obtained by crossing *P[hs83-GFP-JIL-1]/P[hs83-GFP-JIL-1]*; $dGcn5^{sex204}$/*TM6B* to $dGcn5^{E333st}$/*TM6C*.

To obtain overexpressed JIL-1 in animals homozygous for *dAda2a* or *dGcn5* hypomorphic mutations, the following crosses were performed: *P[hs83-GFP-JIL-1]/P[hs83-GFP-JIL-1];* $dAda2a^{d189}$/TM6C to *P[DtlRpb4]; P[DtlAda2a]*$^{79/1}$$dAda2a^{d189}$*/TM6C* and *P[hs83-GFP-JIL-1]/P[hs83-GFP-JIL-1];* $dGcn5^{sex204}$*/TM6B* to $dGcn5^{C137T}$*/TM6B*. The analyzed genotypes were *P[hs83-GFP-JIL-1]/P[DtlRpb4]; P[DtlAda2a]*$^{79/1}$$dAda2a^{d189}$*/*$dAda2a^{d189}$ and *P[hs83-GFP-JIL-1]/+;* $dGcn5^{sex204}/dGcn5^{C137T}$. The control crossings were: $dAda2a^{d189}$/TM6C to *P[DtlRpb4]; P[DtlAda2a]*$^{79/1}$$dAda2a^{d189}$*/TM6C* and $dGcn5^{sex204}$/TM6B to $dGcn5^{C137T}$*/TM6C*. To ensure JIL-1 expression, animals carrying the *P[hs83-GFP-JIL-1]* transgene were heat-treated at 37°C for 30 minutes each day from L1 during 3 or 4 days in each experiment.

To produce *dAda2a*/*dSu(var)3-9* and *dGcn5*/*dSu(var)3-9* double mutants, $dAda2a^{d189}$ or $dGcn5^{sex204}$ and *dSu(var)3-9* alleles were recombined into the same chromosome and the recombinant strains were crossed to *P[DtlRpb4]* $dAda2a^{d189}$/TM6C and $dGcn5^{E333st}$*/TM6C,* respectively. The analyzed genotypes were *dSu(var)3-9* $dAda2a^{d189}$*/ P[DtlRpb4]* $dAda2a^{d189}$ and *dSu(var)3-9* $dGcn5^{sex204}$*/* $dGcn5^{E333st}$.

For rescue experiments the L3 animals identified as non-*Tubby* were gently transferred to new vials, allowed to develop at 25°C analyzed and scored for pupa formation or hatching rate. To determine the sex ratio, homozygous L3 animals carrying the Jll-1 transgene were gently transferred to new vials after differentiating the sexes on the basis of the presence of testes under a dissecting microscope.

Immunohistochemistry

Polytene chromosome spreads obtained from the salivary glands of wandering larvae of the genotype indicated at the Figs were treated with 3.7% formaldehyde dissolved in phosphate-buffered saline (PBS), then incubated in 45% acetic acid for 1 minute. Slides were blocked in PBST (PBS+ 0.1% Tween-20) + 5% fetal calf serum for 1 hour at 25°C and incubated overnight at 4°C in a mixture of primary antibodies. Samples were washed in PBST and incubated with a mixture of secondary antibodies (Alexa-Fluor-555-conjugated anti-rabbit- and Alexa-Fluor-488-conjugated anti-mouse IgGs, Molecular Probes) for 1 hour at 25°C. The slides were incubated with DAPI in PBST for 2 minutes at 25°C, washed again and covered with Fluoromount-G mounting medium (Southern Biotech). Specific polyclonal antibodies against H3S10ph, H3K9me2, H4 acetylated at Lys5 (H4K5ac), H4K12ac were from ABCAM or Upstate and were used at 1:100 or 1:200 dilutions. JIL-1-specific monoclonal antibody (5C9) used at 1:5 dilution was kindly provided by Kristen Johansen. Mouse anti-Pol II (7G5) was provided by Laszlo Tora (IGBMC, Illkirch, France). Secondary antibodies Alexa-Fluor-488-conjugated goat anti-mouse IgG and Alexa-Fluor-555-conjugated goat anti-rabbit IgG (Molecular Probes) were used at 1:500 dilutions.

'Smush' preparations of polytene nuclei from third instar salivary gland were prepared as described (Wang et al., 2001). For immunostaining of larval tissue samples, animals were dissected in PBS and fixed in 4% formaldehyde solution. Treatment with anti-JIL-1 primary antibody (1:5 dilution) at 4°C, was followed by incubation with Alexa-Fluor-488-conjugated anti-mouse secondary antibody (Molecular Probes). Stained samples were examined with an OLYMPUS BX51 microscope and photos were taken with an Olympus DP70 camera using identical settings for mutant and control samples.

Quantitative real-time PCR

For the quantitative determination of *JIL-1* mRNA, total RNA was isolated from 20 L3 larvae by using the RNeasy Mini Kit (Qiagen). First-strand cDNA was synthesized from 1 μg RNA using TaqMan reverse transcription reagent (ABI). Quantitative real-time (RT)-PCR (Q-RT-PCR) was performed following the incorporation of SYBRGreen (using the ABI, 7500 Real Time PCR System) using primers specific

for JIL-1 and for 18S rRNA as a control. C_T values were set against a calibration curve. The $\Delta\Delta C_T$ method was used for the calculation of the relative abundances (Winer et al., 1999). The sequences of specific primers were the following. 18S forward 5′-GCCAGCTAGCAATTGGGTGTA-3′, 18S reverse 5′-CCGGAGCC-CAAAAAGCTT-3′, JIL-1Fw 5′-TGCCCACCAGCAATAGTACA-3′, JIL-1Rev, 5′-GCATACAATTTTCCGGCATC-3′. Each experiment was repeated three to four times.

Western blotting

For protein analysis by immunoblotting total protein samples were extracted from third instar larvae of the genotypes indicated in the figure legends, the concentration was measured using the Bradford reagent, 25 μg protein was separated on SDS-PAGE and transferred by electroblotting to nitrocellulose membrane. The membranes were blocked for 1 h in 5% BSA in TBST (20 mM Tris-HCl, pH 7.4, 150 mM NaCl, 0.05% Tween 20) and incubated overnight with primary antibody diluted in 2% BSA TBST. For the detection of histone H3, H4, H4K12ac and H3S10ph commercially available antibodies (ABCAM) were used. The same membranes developed with H4K12ac or H3S10ph specific polyclonal primary antibodies were washed in TBST and reprobed with anti-H4 monoclonal antibody or anti-H3 polyclonal antibody. Membranes were washed, incubated with horseradish peroxidase-conjugated anti-rabbit or anti-mouse secondary antibodies (DACO), washed again extensively, and developed using the ECL (Millipore) kit following the manufacturer's recommendations.

We are grateful to Cristophe Antoniewski for kindly providing *Gcn5*-mutant stocks as well as *Gcn5* transgenes, and to Laszlo Tora who supplied the Pol II antibody. We are very grateful to Kristen Johansen who provided the JIL-1^{z2} allele, JIL-1EGFP transgene and JIL-1 monoclonal antibody, and who prepared the western blot using anti-JIL-1 antibody. This work was supported by grants from the Hungarian Science Fund (OTKA T046414), the Hungarian Ministry of Health (ETT 078/2007) and EU FP-6 (LSHG-CT-2004-502950). A.C. is a European Community RTN Marie Curie research fellow supported by grant HPRN-CT-2004-504228.

References

Badenhorst, P., Voas, M., Rebay, I. and Wu, C. (2002). Biological functions of the ISWI chromatin remodeling complex NURF. *Genes Dev.* **16**, 3186-3198.

Badenhorst, P., Xiao, H., Cherbas, L., Kwon, S. Y., Voas, M., Rebay, I., Cherbas, P. and Wu, C. (2005). The Drosophila nucleosome remodeling factor NURF is required for Ecdysteroid signaling and metamorphosis. *Genes Dev.* **19**, 2540-2545.

Berger, S. L. (2007). The complex language of chromatin regulation during transcription. *Nature* **447**, 407-412.

Carre, C., Szymczak, D., Pidoux, J. and Antoniewski, C. (2005). The histone H3 acetylase dGcn5 is a key player in Drosophila melanogaster metamorphosis. *Mol. Cell. Biol.* **25**, 8228-8238.

Carre, C., Ciurciu, A., Komonyi, O., Jacquier, C., Fagegaltier, D., Pidoux, J., Tricoire, H., Tora, L., Boros, I. M. and Antoniewski, C. (2007). The Drosophila NURF remodelling and the ATAC histone acetylase complexes functionally interact and are required for global chromosome organization. *EMBO Rep*. **9**, 187-192.

Cheung, P., Tanner, K. G., Cheung, W. L., Sassone-Corsi, P., Denu, J. M. and Allis, C. D. (2000). Synergistic coupling of histone H3 phosphorylation and acetylation in response to epidermal growth factor stimulation. *Mol. Cell* **5**, 905-915.

Ciurciu, A., Komonyi, O., Pankotai, T. and Boros, I. M. (2006). The Drosophila histone acetyltransferase Gcn5 and transcriptional adaptor Ada2a are involved in nucleosomal histone H4 acetylation. *Mol. Cell. Biol.* **26**, 9413-9423.

Deng, H., Zhang, W., Bao, X., Martin, J. N., Girton, J., Johansen, J. and Johansen, K. M. (2005). The JIL-1 kinase regulates the structure of Drosophila polytene chromosomes. *Chromosoma* **114**, 173-182.

Deng, H., Bao, X., Zhang, W., Girton, J., Johansen, J. and Johansen, K. M. (2007). Reduced levels of Su(var)3-9 but not Su(var)2-5 (HP1) counteract the effects on chromatin structure and viability in loss-of-function mutants of the JIL-1 histone H3S10 kinase. *Genetics* **177**, 79-87.

Deng, H., Bao, X., Cai, W., Blacketer, M. J., Belmont, A. S., Girton, J., Johansen, J. and Johansen, K. M. (2008). Ectopic histone H3S10 phosphorylation causes chromatin structure remodeling in Drosophila. *Development* **135**, 699-705.

Deuring, R., Fanti, L., Armstrong, J. A., Sarte, M., Papoulas, O., Prestel, M., Daubresse, G., Verardo, M., Moseley, S. L., Berloco, M. et al. (2000). The ISWI chromatin-remodeling protein is required for gene expression and the maintenance of higher order chromatin structure in vivo. *Mol. Cell* **5**, 355-365.

Ebert, A., Schotta, G., Lein, S., Kubicek, S., Krauss, V., Jenuwein, T. and Reuter, G. (2004). Su(var) genes regulate the balance between euchromatin and heterochromatin in Drosophila. *Genes Dev.* **18**, 2973-2983.

Eggert, H., Gortchakov, A. and Saumweber, H. (2004). Identification of the Drosophila interband-specific protein Z4 as a DNA-binding zinc-finger protein determining chromosomal structure. *J. Cell Sci.* **117**, 4253-4264.

Grau, B., Popescu, C., Torroja, L., Ortuno-Sahagun, D., Boros, I. and Ferrus, A. (2008). Transcriptional adaptor ADA3 of Drosophila melanogaster is required for histone modification, position effect variegation, and transcription. *Mol. Cell. Biol.* **28**, 376-385.

Guelman, S., Suganuma, T., Florens, L., Swanson, S. K., Kiesecker, C. L., Kusch, T., Anderson, S., Yates, J. R. 3rd, Washburn, M. P., Abmayr, S. M. et al. (2006). Host cell factor and an uncharacterized SANT domain protein are stable components of ATAC, a novel dAda2A/dGcn5-containing histone acetyltransferase complex in Drosophila. *Mol. Cell. Biol.* **26**, 871-882.

Ito, T. (2007). Role of histone modification in chromatin dynamics. *J. Biochem.* **141**, 609-614.

Jin, Y., Wang, Y., Walker, D. L., Dong, H., Conley, C., Johansen, J. and Johansen, K. M. (1999). JIL-1: a novel chromosomal tandem kinase implicated in transcriptional regulation in Drosophila. *Mol. Cell* **4**, 129-135.

Jin, Y., Wang, Y., Johansen, J. and Johansen, K. M. (2000). JIL-1, a chromosomal kinase implicated in regulation of chromatin structure, associates with the male specific lethal (MSL) dosage compensation complex. *J. Cell Biol.* **149**, 1005-1010.

Johansen, K. M. and Johansen, J. (2006). Regulation of chromatin structure by histone H3S10 phosphorylation. *Chromosome Res.* **14**, 393-404.

Komonyi, O., Papai, G., Enunlu, I., Muratoglu, S., Pankotai, T., Kopitova, D., Maroy, P., Udvardy, A. and Boros, I. (2005). DTL, the Drosophila homolog of PIMT/Tgs1 nuclear receptor coactivator-interacting protein/RNA methyltransferase, has an essential role in development. *J. Biol. Chem.* **280**, 12397-12404.

Labrador, M. and Corces, V. G. (2003). Phosphorylation of histone H3 during transcriptional activation depends on promoter structure. *Genes Dev.* **17**, 43-48.

Lee, K. K. and Workman, J. L. (2007). Histone acetyltransferase complexes: one size doesn't fit all. *Nat. Rev. Mol. Cell. Biol.* **8**, 284-295.

Li, B., Carey, M. and Workman, J. L. (2007). The role of chromatin during transcription. *Cell* **128**, 707-719.

Lo, W. S., Trievel, R. C., Rojas, J. R., Duggan, L., Hsu, J. Y., Allis, C. D., Marmorstein, R. and Berger, S. L. (2000). Phosphorylation of serine 10 in histone H3 is functionally linked in vitro and in vivo to Gcn5-mediated acetylation at lysine 14. *Mol. Cell* **5**, 917-926.

Oki, M., Aihara, H. and Ito, T. (2007). Role of histone phosphorylation in chromatin dynamics and its implications in diseases. *Subcell. Biochem.* **41**, 319-336.

Pankotai, T., Komonyi, O., Bodai, L., Ujfaludi, Z., Muratoglu, S., Ciurciu, A., Tora, L., Szabad, J. and Boros, I. (2005). The homologous Drosophila transcriptional adaptors ADA2a and ADA2b are both required for normal development but have different functions. *Mol. Cell. Biol.* **25**, 8215-8227.

Papai, G., Komonyi, O., Toth, Z., Pankotai, T., Muratoglu, S., Udvardy, A. and Boros, I. (2005). Intimate relationship between the genes of two transcriptional coactivators, ADA2a and PIMT, of Drosophila. *Gene* **348**, 13-23.

Rath, U., Ding, Y., Deng, H., Qi, H., Bao, X., Zhang, W., Girton, J., Johansen, J. and Johansen, K. M. (2006). The chromodomain protein, Chromator, interacts with JIL-1 kinase and regulates the structure of Drosophila polytene chromosomes. *J. Cell Sci.* **119**, 2332-2341.

Rea, S., Eisenhaber, F., O'Carroll, D., Strahl, B. D., Sun, Z. W., Schmid, M., Opravil, S., Mechtler, K., Ponting, C. P., Allis, C. D. et al. (2000). Regulation of chromatin structure by site-specific histone H3 methyltransferases. *Nature* **406**, 593-599.

Reuter, G., Dorn, R., Wustmann, G., Friede, B. and Rauh, G. (1986). Third chromosome suppressor of position-effect variegation loci in Drosophila melanogaster. *Mol. Gen. Genet.* **202**, 481-487.

Ryder, E., Ashburner, M., Bautista-Llacer, R., Drummond, J., Webster, J., Johnson, G., Morley, T., Chan, Y. S., Blows, F., Coulson, D. et al. (2007). The DrosDel deletion collection: a Drosophila genomewide chromosomal deficiency resource. *Genetics* **177**, 615-629.

Schotta, G., Ebert, A., Krauss, V., Fischer, A., Hoffmann, J., Rea, S., Jenuwein, T., Dorn, R. and Reuter, G. (2002). Central role of Drosophila SU(VAR)3-9 in histone H3-K9 methylation and heterochromatic gene silencing. *EMBO J.* **21**, 1121-1131.

Spierer, A., Seum, C., Delattre, M. and Spierer, P. (2005). Loss of the modifiers of variegation Su(var)3-7 or HP1 impacts male X polytene chromosome morphology and dosage compensation. *J. Cell Sci.* **118**, 5047-5057.

Suganuma, T., Gutierrez, J. L., Li, B., Florens, L., Swanson, S. K., Washburn, M. P., Abmayr, S. M. and Workman, J. L. (2008). ATAC is a double histone acetyltransferase complex that stimulates nucleosome sliding. *Nat. Struct. Mol. Biol.* **15**, 364-372.

Swaminathan, J., Baxter, E. M. and Corces, V. G. (2005). The role of histone H2Av variant replacement and histone H4 acetylation in the establishment of Drosophila heterochromatin. *Genes Dev.* **19**, 65-76.

Tschiersch, B., Hofmann, A., Krauss, V., Dorn, R., Korge, G. and Reuter, G. (1994). The protein encoded by the Drosophila position-effect variegation suppressor gene Su(var)3-9 combines domains of antagonistic regulators of homeotic gene complexes. *EMBO J.* **13**, 3822-3831.

Wang, Y., Zhang, W., Jin, Y., Johansen, J. and Johansen, K. M. (2001). The JIL-1 tandem kinase mediates histone H3 phosphorylation and is required for maintenance of chromatin structure in Drosophila. *Cell* **105**, 433-443.

Winer, J., Jung, C. K., Shackel, I. and Williams, P. M. (1999). Development and validation of real-time quantitative reverse transcriptase-polymerase chain reaction for monitoring gene expression in cardiac myocytes in vitro. *Anal. Biochem.* **270**, 41-49.

Zhang, W., Jin, Y., Ji, Y., Girton, J., Johansen, J. and Johansen, K. M. (2003). Genetic and phenotypic analysis of alleles of the Drosophila chromosomal JIL-1 kinase reveals a functional requirement at multiple developmental stages. *Genetics* **165**, 1341-1354.

Zhang, W., Deng, H., Bao, X., Lerach, S., Girton, J., Johansen, J. and Johansen, K. M. (2006). The JIL-1 histone H3S10 kinase regulates dimethyl H3K9 modifications and heterochromatic spreading in Drosophila. *Development* **133**, 229-235.

Zhimulev, I. F. (1996). Morphology and structure of polytene chromosomes. *Adv. Genet.* **34**, 1-497.